©2015

Ryan W. Hupfer

THE EFFECT OF LAKE LEVEL ON SULFUR ISOTOPE SYSTEMATICS IN THE

LOCKATONG FORMATION OF THE NEWARK BASIN, NEW JERSEY

By

Ryan W. Hupfer

A thesis submitted to the

Graduate School – New Brunswick

Rutgers, The State University of New Jersey

in partial fulfillment of the requirements

for the degree of

Master of Science

Graduate Program in Geological Sciences

written under the direction of

James D. Wright and John R. Reinfelder

And approved by

_____

_____

_____

New Brunswick, New Jersey

October, 2015

ABSTRACT OF THE THESIS

The effect of lake level on sulfur isotope systematics in the Lockatong Formation of the

Newark Basin, New Jersey

By: Ryan W. Hupfer

Thesis Directors:

Dr. James D. Wright and Dr. John R. Reinfelder

The Lockatong Formation is composed of lacustrine sediments that were

deposited in the Newark Basin during the Late Triassic (~222-218 Ma). This formation

is characterized by black, organic rich layers interspersed with iron-oxide rich, red layers

at various intervals, both of which contain pyrite, indicating that the lake supported a

community of sulfate reducing bacteria. The stratigraphic patterns of this formation

reflect cyclic depositional environments of the ancient lake from a deep, productive

freshwater lake to a playa or completely dried out lake bed. Wet-dry cycles forced by

climatic changes are proposed as the primary influence on the sulfate concentration in the

paleo-lakes of the Newark Basin, which influences the δ^{34}S of sulfide, produced from

bacterial sulfate reduction and is preserved in pyrite.

In modern closed systems, stratification influences sulfate concentration. Deep

lakes with euxinic bottom waters have sulfate concentrations that limit bacterial sulfate

reduction producing sulfide with high δ^{34}S values, which are preserved in sedimentary

pyrite. Conversely, low lake levels have a higher sulfate concentration, resulting in more

fractionation and lower $\delta^{34}S$ values. This study tests this hypothesis using the varying lake levels in the Triassic Newark Basin. Comparison of $\delta^{34}S$ values from pyrite and sedimentary depth rankings show that deep lake pyrite samples have relatively high $\delta^{34}S$ values (+5 ± 5 ‰) while shallow lake deposits have lower values (-6‰ ± 5 ‰). These findings indicate a relationship between climatically controlled lake level and $\delta^{34}S$ values that are preserved in sedimentary pyrite.

ACKNOWLEDGEMENTS

TABLE OF CONTENTS

LIST OF TABLES

LIST OF FIGURES

1. Introduction

Sulfur cycling in aquatic systems is controlled by a balance between biologically-driven and abiotic oxidation and reduction reactions (Jørgensen 1988, 1990). Many studies have examined the modern lacustrine sulfur cycle (Holmer & Storkholm, 2001); however, lake environments can vary substantially over time due to tectonics, sedimentary processes, and climate (Olsen et al., 1996). Large lakes undergo transitions from having a deep, well-stratified water column to becoming a shallow, well-mixed water body, a playa, or even drying out in a few decades to thousands of years. Understanding the freshwater sulfur cycle is important because biotic and abiotic reactions of sulfur influence the cycling of carbon, nitrogen, phosphorous, and iron, all important elements in natural systems. Changes in lake depth affect redox conditions, indicated by trace metal geochemistry (Zhu, 2010). What then, are the effects of such lake depth-driven redox changes on major elements?

For sulfur, lower redox potentials in the sediments of lakes during periods when the water column is relatively deep may support the production of pyrite. Pyrite formation requires sulfate (SO_4^{2-}) to be reduced to sulfide (S^{2-}), which is catalyzed by bacterial sulfate reduction (BSR) (Rickard, 1969). BSR causes a significant kinetic fractionation of sulfur isotopes; the S^{2-} produced from BSR is depleted in ^{34}S as bacteria preferentially reduce the lighter isotope ^{32}S relative to the sulfate concentration in the water column. This fractionation decreases the $^{34}S/^{32}S$ ratio in biologically produced S^{2-} than in the SO_4^{2-} source, which becomes enriched in ^{34}S (Jones & Starkey, 1957;

Harrison & Thode, 1958; Kaplan & Rittenburg, 1964). Sulfur isotope ratios are represented as a difference in thousandths or "per mil" (‰) with respect to a standard in delta notation:

$$\delta^{34}S\ (‰) = [((^{34}S/^{32}S)\ sample/\ (^{34}S/^{32}S)\ standard)-1]*1000 \quad (1)$$

BSR produces a large range of sulfur isotopic discrimination factors (approximately equal to the difference in $\delta^{34}S$ values) between reactant, SO_4^{2-}, and product, S^{2-} (4‰ - 46‰). This range reflects variations in environmental parameters controlling the biological sulfur cycle including SO_4^{2-} concentration (Harrison & Thode, 1958; Rees, 1972), water temperature, type of organic substrate (Kaplan & Rittenburg, 1964; Kemp & Thode, 1968; Chambers et al., 1975) and amount of organic substrate (Canfield, 2000). These factors affect sulfur isotope fractionation by influencing the sulfate reduction rate (SRR); the highest fractionations are measured at the lowest SRR (Harrison & Thode 1958). Since all of these parameters can vary with changes in hydrology, the $\delta^{34}S$ of lacustrine pyrite in sedimentary rocks and large scale climate forcing are expected to be related.

1.1. Goals for this work

Sulfide minerals produced from BSR have distinct $\delta^{34}S$ values. The isotope discrimination factor between the oxidized and reduced sulfur species depends on the SRR which is primarily dependent on the availability of sulfate (Harrison & Thode, 1958; Canfield, 2000). The dominant source of sulfur in lacustrine settings comes from the weathering of rocks containing sulfur minerals and the oxidation of terrestrial organic sulfur (Holmer & Storkholm, 2001). It is widely known that the presence of water

enhances chemical weathering rates (Yatsu, 1988). Sulfate concentrations in closed

basins are therefore dependent on the availability of water to exposed rocks, therefore

there should be some relationship between precipitation and $\delta^{34}S$ values of lacustrine

pyrite. While some studies have looked at sulfur isotope systematics in modern

freshwater systems with high (Zerkle et al., 2010) and low (Gomes & Hurtgen, 2013;

2015) SO_4^{2-} concentrations, no known studies have taken an in-depth look at their link to

the astronomical cycles and their response to climate change and fluctuations in lake

level.

Two possible relationships between $\delta^{34}S$ values of pyrite and lake depth in the

Triassic Newark Basin are possible: (1) $\delta^{34}S$ will become remain constant with increasing

lake depth because of the continual addition of sulfate from run off, or (2) $\delta^{34}S$ values

will increase with increasing lake depth because of the effect of the low sulfate

concentration associated with a highly reducing environment and the effect on the

fractionation associated with BSR. An examination of the sulfur cycle in a rift basin lake

system will lead to an improved understanding of how climate affects lacustrine

geochemistry and the fresh water sulfur cycle.

This thesis uses the well-established stratigraphic framework (Olsen & Kent,

1995) and lake level records of the Newark Basin (Olsen, 1984b; 1986; Olsen & Kent,

1995; Olsen et al., 1996) to investigate the effects of the astronomically paced wet-dry

cycles on sulfur biogeochemistry in Triassic rift basin lakes. The 6,770 m of core from

the Newark Basin Coring Project (NBCP) span approximately 30 million years (Olsen et

al., 1996) and provide a continuous climate and water depth record for the lake that once

filled this rift basin. This study focuses on a 21 m section of core from the Lockatong

formation that includes two high stands (dark gray and black mudstones) and two low stands (red and purple mudstones) across two Van Houten cycles, which were deposited over approximately 42 kyr. Using a compiled record of pyrite $\delta^{34}S$ values the known tempo of climate forcing, this study examines the effect of lake level fluctuation on the sulfur cycle.

2. Geologic History & Setting

2.1. Geologic History

The Lockatong Formation is composed of Late Triassic (~218-222 Ma) lacustrine sediments that were deposited in the Newark Basin, a closed basin lake in one of the many Mesozoic extensional basins of eastern North America (Figure 1) (Olsen, 1978; Manspeizer, 1982). Footwall collapse of the basin during the initial stages of the breakup of Pangea forced a change in the hydrologic regime from fluvial, which can be seen in the Stockton formation, to lacustrine, setting the stage for the deposition of the fine grained sediments of the Lockatong formation (Schlische, 1992). Changes in the thicknesses of sedimentary packages in the Lockatong reveal that in addition to extension, the Newark Basin had also undergone syn-depositional, intra-basinal faulting and folding (Schlische, 1992). Tilting and folding occurred until ~175 Ma, after which the rocks were weathered and eroded from the Middle Jurassic to the Early Cretaceous (Witte & Kent, 1991). In the Early Cretaceous high sea levels and flexural loading caused the sediments of the coastal plain to onlap onto the Newark Basin rocks, shielding them from further erosion (Schlische, 1992).

2.2. Geologic Setting

The sedimentary deposits of the Lockatong formation are characterized by black, organic rich layers interspersed with red, iron-oxide rich layers at various intervals. The presence of pyrite in both the dark and light facies of the Lockatong indicates that biological sulfur cycling was active in the Triassic lake. Whole rock trace metal geochemistry indicates that the changes in lake level were large enough to be linked to changes in redox conditions in the lake (Zhu, 2010). Light red, purple, gray, and white sedimentary units represent shallow lake levels and oxidizing conditions that persisted during arid times and dark gray, purple, and black units represent deeper lake levels and reducing conditions that persisted during humid intervals (Olsen et al., 1996; Zhu, 2010). The changes in redox conditions are possibly because of stratification of the water column in the paleolake. Assuming that the paleolake was similar to modern environments such as Lake McCarrons, Minnesota, USA (Gomes & Hurtgen, 2013) and Framvaren Fjord, Norway (Sælen et al., 1993), when the lake was shallow, there was a well-mixed, oxic water column and when the lake was deep there was a stratified water column with anoxic bottom waters.

Early investigations noted stratigraphic patterns in the lacustrine and fluvial strata of the in the Lockatong formation (McLaughlin, 1933; 1946b; Van Houten, 1964). These patterns reflect variations in the depositional environment of the ancient lake, as water depth oscillated between about 100 m (productive freshwater lake) to nearly 0 m (playa or completely dried out lake bed) (Olsen, 1984b). Large changes in lake level are thought to have been governed by cloud cover and the amount of precipitation in the rift

valley (Benson, 1981; Olsen, 1984). Further investigation demonstrated that the patterns seen in the Lockatong were also observed in the Passaic Formation (Olsen, 1986).

The periods of these oscillations have been linked to the precession (~20 kyr) and eccentricity (~100 kyr, 413 kyr, 2 Myr) cycles of Earth's orbit and the associated climatic effects (Van Houten, 1964; Olsen & Kent, 1995). Four types of cycles are recognized in the Newark Basin: (1) the Van Houten Cycle, (2) the short modulating cycle, (3) the McLaughlin cycle, and (4) the long modulating cycle (Olsen & Kent, 1995; Olsen et al., 1996).

Van Houten cycles are typically made up of three different sedimentary facies: (1) a thin, massive, unit that becomes more laminated up-section as the occurrence of desiccation cracks and root burrows decreases and represents lake transgression, (2) a fissile gray to black mudstone that exhibits well defined bedding that becomes more massive up-section and represents lake high level stand, and (3) a unit that becomes more massive up-section as the occurrence of desiccation cracks and root burrows increases and represents lake regression (Olsen, 1986). Facies (1) and (3) can be red, purple, or gray; typically a lighter variety. Facies (2) is typically a dark color and can be red, purple, gray, or black (Olsen et al., 1996). Evaporite pseudomorphs can be found in the upper reaches of facies (2) and throughout facies (3) (El Tabakh, 1994). Van Houten cycles record the rise and fall of the lake level by precipitation variation associated with the ~ 20,000 yr. precession cycles.

Van Houten cycles are modulated by short and long cycles. Short modulation cycles are composed of 4 to 6 (usually 5) Van Houten cycles that vary in their degree of

lamination and amount of black and dark colored facies (Olsen et al., 1996). Short
modulating cycles are the climatic expression of the 95,000 and 125,000 year cycles of
the eccentricity of Earth's orbit (Olsen and Kent, 1995).

McLaughlin cycles are made up of 4 short modulation cycles that show similar
variations to those of Van Houten cycles (Olsen et al., 1996). Of all of the compound
cycles, the McLaughlin cycles are the strongest and the 53 primary divisions of the
Lockatong and Passaic formations are McLaughlin cycles, representing ~ 400 kyr (Olsen
and Kent, 1995).

The base of a McLaughlin cycle is marked by the darkest facies associated with
the Van Houten cycles; whereas at the middle to upper reaches of a McLaughlin cycle
red, light gray, and white facies are more abundant (Olsen et al., 1996). McLaughlin
cycles are a climatic expression of the 413,000 year cycle of Earth's orbital eccentricity
(Olsen et al., 1996). Long modulating cycles are mostly composed of 4 or 5 McLaughlin
cycles. As with the other cycles, dark and gray facies dominate the bottoms of the cycles
and red and buff facies dominate the tops (Olsen et al., 1996). Long modulating cycles
may be the climatic expression of the 2 Myr orbital eccentricity cycle.

3. Lacustrine Sulfur Cycle

3.1. Sulfur Cycle Systematics

The global sulfur cycle has three main reservoirs: SO_4^{2-} in the oceans, SO_4^{2-} in
evaporites, and S^{2-} which is found mostly in pyrite (Figure 2). Wet deposition of
volcanic emissions and the weathering of rocks with sulfide and sulfate minerals are the

primary sources of sulfur to the ocean while the formation of sulfide and sulfate minerals are the primary sinks (Newton & Bottrell, 2007). The sulfur cycle in lakes has some similarities to the global cycle, but in many ways operates differently than the world's oceans (Figure 3).

Most of the sulfur in lakes comes from the weathering of rocks containing sulfur minerals and the oxidation of organic sulfur from terrestrial sources (Holmer & Storkholm, 2001), a primary assumption that is applied to the Triassic Lake for this study. The overlying water is the main source of sulfur to sediments. Once in the sediments, SO_4^{2-} undergoes assimilatory and dissimilatory bacterial sulfate reduction (BSR). While assimilatory SO_4^{2-} reduction results in the production of organic S compounds used in cells, dissimilatory SO_4^{2-} reduction uses SO_4^{2-} as a terminal electron acceptor during the biological oxidation of organic matter producing H_2S. Dissimilatory BSR is the dominant pathway of SO_4^{2-} reduction in marine sediments, but is also important in some lacustrine systems. In freshwater sediments, sulfate reducing bacteria (SRB) are dominated by gram-negative Deltaproteobacteria (Devereaux et al., 1989) and while SO_4^{2-} is the primary electron acceptor, most SRB can also use a variety of electron acceptors such as thiosulfate ($S_2O_3^{2-}$), sulfite (SO_3^{2-}), elemental sulfur (S^0), and nitrate (NO_3^-) (Holmer & Storkholm, 2001). While pure-culture experiments have suggested that SO_4^{2-} reduction can only occur under anoxic conditions, it has been observed in the well-oxygenated photosynthesis zone in hypersaline bacterial mats (Canfield & Des Marais, 1991). Furthermore SRB have been isolated from both oxic and anoxic sediment (Jørgensen & Bak, 1991). These findings indicate that in nature, SRB can survive to some extent under oxic conditions (Sass et al., 1997; Eschmann et al., 1999). Some SRB

can also consume O_2 via respiration (Dilling & Cypionka, 1990; Marschall et al., 1993) which may allow them to survive under oxic conditions. BSR may therefore occur in both oxic and anoxic environments.

Some SRB are capable of disproportionation of intermediate oxidation states of sulfur. For example, certain bacteria have a metabolism that can split $S_2O_3^{2-}$, SO_3^{2-}, or S^0 into two new compounds, one more reduced and one more oxidized than the original substrate, to gain energy (Bak & Cypionka, 1987; Janssen et al., 1996). It is estimated that 44% of $S_2O_3^{2-}$ added to sediments is disproportionated (Jørgensen, 1990), indicating that disproportionation of sulfur intermediates is an important process in lake sediments.

While the main source of SO_4^{2-} to sediments is from the overlying water, biological and chemical processes in the sediments provide additional sources, albeit minor. Hydrolysis of sedimentary sulfate-esters contributes about 10% of sedimentary SO_4^{2-} (King & Klug, 1982a). Re-oxidation of sulfur compounds has also been found to increase the supply of SO_4^{2-} to the sediments (Bak & Pfenning, 1991) and the rate of BSR (Jørgensen, 1990).

The relative importance of the organic sulfur sink is the major difference between lacustrine and marine environments. In lacustrine settings it is estimated that 53% of reduced sulfur is initially incorporated into organic compounds (Rudd et al., 1986). The remaining 47% of reduced S^{2-} forms S^0, pyrite, and pyrite precursors in the sediment. It is estimated that 43% and 63% of organic and inorganic sulfur, respectively, is oxidized back to sulfate. Thus 57% of reduced S is stored in lake sediments in the organic form.

Of the sulfate that is reduced in lake sediment 53% is oxidized back to SO_4^{2-} and returns to the water column (Figure 4) (Rudd et al., 1986).

3.2. Sulfur reservoirs and S isotope systematics

The primary sources of sulfur to the Triassic lakes were runoff and deposition of volcanic emissions (Figure 3). In the Newark Basin during the Late Triassic, the Appalachian highlands could have acted as a hydrologic source to the west of the Triassic lake (Pazzaglia & Brandon, 1996). Sulfate and sulfide minerals in the Appalachians have high $\delta^{34}S$ values with most values ranging from +20 to +30 ‰ (Ault & Kulp, 1960; Howe, 1981; Crawford & Beales, 1983; LeHuray, 1984; Wilbur et al., 1990; Appold et al., 1995). In contrast, volcanic emissions typically have $\delta^{34}S$ values of 0‰ (Holser et al., 1988; Newton & Bottrell, 2007).

The reservoirs of sulfur in the Triassic lake were aqueous SO_4^{2-} and H_2S in the water column and sediment pore water and pyrite and its precursors, $S_2O_3^{2-}$ SO_3^{2-}, S^0, and organic S compounds in the sediments (Figure 3). Due to the sulfur isotope signature of the minerals in the local rocks, SO_4^{2-} in the Triassic lake probably had a high isotope value (+20 to +30 ‰). By extension, biologically produced S^{2-} would have had high $\delta^{34}S$ values relative to marine environments. While the formation of organic sulfur compounds in the sediment is an important process, this process is not associated with sulfur isotope fractionation (Nriagu & Soon, 1985). The re-oxidation and disproportionation of sulfide and sulfur intermediates ($S_2O_3^{2-}$ SO_3^{2-}, S^0) can impart a wide range of fractionations from 0‰ to 28±7 ‰ (Ivanov et al., 1976; Fry et al., 1984; Fry et al., 1985; Fry et al., 1986; Habicht et al., 1998) (Figure 5); however, sulfur intermediates

are not considered a large sulfur reservoir (Holmer and Storkholm, 2001) and therefore

would not significantly affect the sulfur isotope values preserved in pyrite.

4. Materials and Methods

4.1 Pyrite sampling

The pyrite samples used in this study were obtained from the Nursery #1 core

from Ewing, New Jersey (Figure 6), which was collected as part of the Newark Basin

Coring Project (Olsen et al., 1996). The Newark Basin Coring Project targeted the center

of the Newark Basin paleolake to recover the most complete record of the lake

sequences. This strategy also benefits this study because the full sulfur cycle will only be

recorded in the deepest parts of the lake because it records the deepest lake depths and

therefore the large scale changes. A core from the distal parts of the lake will not record

the deepest lake depths and therefore will record only the well-mixed oxic conditions.

An interval of 20.76 m, from 908.24 m to 929 m, was examined and sampled. This

length was chosen to include samples from two high lake level intervals and two low lake

level intervals, or two Van Houten cycles. The Nursery #1 core was sampled at 24

different depths where pyrite was visible at the core surface (Figure 7). The sample

spacing varied from 0.3 m to 2.65 m with most samples having a distance of 1 m or less

to the next sample. Sample depths were dependent upon several factors: (1) the presence

of visible pyrite in the mudstone, (2) locations of other samples, (3) signs of sediment re-

working, and (4) the presence of evaporite pseudomorphs. Sediment containing pyrite

that has been reworked would not be representative of the system at the time of

deposition and evaporite pseudomorphs may contain sulfur and, if present in a large

enough amount, bias sulfur isotope results. In the areas where no pyrite was visible, especially in the dark gray and black shales that were deposited in low sulfate environments, it is possible that very fine pyrite crystals are present that cannot be seen, even with a binocular microscope.

No previous studies have examined the sulfur isotopic composition of pyrite in consolidated lacustrine sediment. Therefore, the following protocol was developed to isolate pyrite from the consolidated rock core. Subsequent to identifying sample locations, pyrite bearing mudstone samples were extracted using a drill press. Cylindrical samples of approximately 3 cm^3 (1.27 cm diameter, 2.54 cm height) were extracted from the core and stored in plastic sample bags for further processing. Samples were next coarsely crushed with a hammer and then more finely crushed using a mortar and pestle. The fine grained residual was examined under a microscope and pyrite grains were picked from the residual using tweezers and a brush. Samples with large pyrite grains (> 2 mm in some cases) were ground further (Figure 8a). Most samples contained fine grained pyrite (< 1mm) (Figure 8b) and no further processing was necessary. Pyrite samples were then stored in individual vials until further analysis.

Previous studies have revealed that most of the sulfur in black and dark gray mudstones resides in pyrite (Zhu, 2010). However, the amount of pyritic sulfur in red mudstone is not well constrained. Whole rock geochemistry indicates that Lockatong red mudstone contains less than 0.15 wt% total sulfur, much less than black and gray mudstones from the Lockatong which typically contain upwards of 0.2 wt% (Zhu, 2010). Mudstone matrix contains little sulfur compared to the pyrite grains; nonetheless, extra care was taken to isolate pyrite in all samples, both red and black, to minimize the

amount of matrix included in the sample portion allocated for isotope analysis. Aside from pseudomorph contamination of the sample, having matrix in a sample decreases the percent weight of sulfur which could cause the sample to lack a sufficient amount of sulfur for reliable sulfur isotope analysis.

Where necessary, pyrite grains (approximately 5 – 30) from each sample were pooled for further analysis. The sedimentation rate is estimated to be 0.5 mm y^{-1} (20.76 m deposited over ~42 kyr) and therefore, the 1.27 cm diameter plug from which the pyrite grains were sampled suggested that each sample level represents approximately 25 years. Lakes can have annual to decadal fluctuations; however, pyrite formation can take several years (Berner, 1970). Therefore, pyrite formation time and sample pooling would yield an average δ^{34}S value for the rock sample. While higher sampling precision might be required for other purposes, a 25-year average sample eliminates some of the annual to decadal fluctuations that might obscure the long-term climate trends. Pyrite grain size is also important to consider. A smaller grain may have a different δ^{34}S value than a large grain formed in the same environment as a small grain records a smaller time interval as it was formed more quickly than the large grain. While this is important to note, in this study, grains were grouped regardless of grain size, therefore, analysis of the pyrite would yield an average δ^{34}S value for all of the pyrite in the cylindrical samples.

4.2 Sulfur Isotope Analysis

Ground pyrite samples and sulfur standards were weighed, with weights ranging from 0.1 – 0.2 mg, loaded into tin capsules, and folded into balls. δ^{34}S values of the pyrite samples were determined using Continuous Flow Isotope Ratio Mass Spectrometry

(CF-IRMS) at the Rutgers University Stable Isotope Lab. The lab at Rutgers University

hosts a Eurovector elemental analyzer with a GVI Isoprime CF-IRMS. Samples were

flash combusted in the mass spectrometer at $1030°C$ on a quartz reactor with tungsten

oxide on alumina and pure reduced copper wires to convert the sulfur to SO_2 for isotope

analysis.   Two or more groups of pyrite from each sample were analyzed to obtain a

repeatable, reliable $\delta^{34}S$ measurement. In some cases up to five different groups of pyrite

from a sample had to be analyzed to get a reliable measurement. This was probably due

to insufficient sulfur in the ground pyrite being analyzed most likely because of

impurities in the pyrite or inclusion of matrix in the sample.

IAEAS-1 (silver sulfide) and NBS 127 (barium sulfate) standards were used in

this study having $\delta^{34}S$ values of -0.3 ‰ and 20.3 ‰ relative to Canyon Diablo Troilite

(CDT), respectively. A pattern of running two standards, one each of, IAEAS-1 and NBS

127, one blank, and six samples was followed to prevent sulfur build up in the vacuum

tubes and to correct for any drift in the machine over time. The analytical drift for each

set of six samples was calculated using the average drift (difference between measured

standard value and known standard value) for the measured values of IAEAS-1 and NBS

127 before and after sample analysis. The IAEAS-1 reference standard was used to

correct $\delta^{34}S$ values for the pyrite samples to the CDT isotope standard, since silver sulfide

was considered to be more representative of pyrite than barium sulfate. Instrumental

precision of the mass spectrometer as assessed on the IAEAS-1 standards was ± 0.2‰ (1

σ). The measurements in this study are reported as parts per thousand (‰) relative to

CDT.

4.3. Depth Rankings

The relative lake level during the time of deposition of the sediment within which each pyrite sample was formed, or the depth rank, was determined using data from previous work on cores from the Newark Basin (Olsen & Kent, 1996). Depth ranks are a semi-quantitative classification which takes into account the grain size of sediments and the structures and textures observed within a sedimentary package. In the Triassic lake, the depth rank scale ranges from 0 to 5. A depth rank of 0 indicates a sediment package deposited in a playa or a shallow lake that frequently dried out. A depth rank of 5 indicates a sediment package deposited in a deep lake, which in the case of the Triassic Lake, could have been greater than 100 m deep (Table 1) (Olsen & Kent, 1996). For example, sample NB30 taken at 915.42 m was from a gray, laminated mudstone, indicating that it formed in a relatively deep lake environment (depth rank 2.5) whereas sample NB 33 taken at 916.18 meters was from a light gray, massive mudstone, indicating a relatively shallow lake environment (depth rank 0). Depth rankings for the Nursery #1 core were obtained from the Newark Basin Coring Project online database (http://www.ldeo.columbia.edu/~polsen/nbcp/nbcp.html). The depth rankings from the database were confirmed by cross-referencing them to depth rankings carried out in this study that were based on the criteria used in the original study (Olsen & Kent, 1996). In areas where there was a sample, but no proximal depth ranking in the database, a depth ranking was made using the original criteria.

5. Results

δ^{34}S values for pyrite from Newark Basin Triassic mudstones range from -11.2‰ to +19.4‰ (Table 2, Figure 9). The error bars on Figure 9 represent the range of δ^{34}S values in multiple pyrite grains from the same sample. Excluding one sample, pyrite formed at deep lake depths (depth ranks > 1) had δ^{34}S values of +5 ± 5‰ (Table 2, Figure 9). With one exception, pyrite formed at shallow lake depths (depth ranks ≤ 1) have δ^{34}S values of ~ -6‰ ± 5 ‰ (Table 2, Figure 9).

The depth rankings show a "saw-toothed" pattern; changes from shallow to deep are abrupt while changes from deep to shallow are gradual. In the upper lake cycle (~916 to 908 m), the δ^{34}S values show a similar pattern, with a sharp increase in values corresponding to the sharp increase in depth ranking. δ^{34}S values then slowly decreased as the depth rankings decreased (Figure 9). For the lower lake cycle (~929 to 916 m), pyrite was not recovered in sufficient quantities in the interval with the highest depth rankings to verify this observation. However, there is a gradual decrease in δ^{34}S values for the upper half of this cycle (Figure 9).

6. Discussion

The δ^{34}S values from pyrite show correspondence with lake depth at the time of formation. The maximum δ^{34}S values for the pyrite samples are suggestive that the source of sulfur supplied to the lake was derived from the weathering of evaporites and sulfide minerals in the Appalachian highlands with δ^{34}S values ranging from +20 to +30‰ (Ault & Kulp, 1960; Howe, 1981; Crawford & Beales, 1983; LeHuray, 1984; Wilbur et al., 1990; Appold et al., 1995). The highest δ^{34}S values are associated with

pyrite formed in intermediate to deep lake conditions, while lower $\delta^{34}S$ values are associated with pyrite formed in shallow lake to playa conditions.

This observation may seem counter-intuitive at first. Dark colored muds are usually rich in organic matter and associated with deep water, euxinic (anoxic, H_2S-rich), and reducing conditions, and light colored muds are usually limited in organic matter and associated with shallow water, oxidizing conditions. A logical conclusion is that BSR would occur unimpeded in a reducing environment rife with organic matter, producing the largest fractionation between the source SO_4^{2-} and produced S^{2-}. However, in deep, semi-closed to closed basins where euxinic and reducing conditions prevail, pyrite with relatively high $\delta^{34}S$ values can form because of the limited supply of SO_4^{2-} (Sælen et al., 1993; Zerkle et al., 2010; Gomes & Hurtgen, 2013; 2015).

In open, SO_4^{2-} rich systems, such as the ocean, SO_4^{2-} is continuously replenished. Closed, SO_4^{2-} poor systems such as marine settings isolated by a sill or deep lakes with euxinic zones have been shown to have different isotope systematics than those of open systems. In closed systems such as Framvaren Fjord, Norway, Lake McCarrons, Minnesota, U.S.A. or Fayetteville Green Lake, New York, U.S.A., stratification can be strong. In these settings, bottom water circulation is either limited or does not occur at all, creating euxinic conditions.

The $\delta^{34}S$ of sulfide preserved in sediment represents the average $\delta^{34}S$ of the sulfide in the water column. In an open system, SRB will consume SO_4^{2-}, and since SO_4^{2-} is continually renewed at all depths isotope values of the sulfide produced from BSR are relatively constant at all depths do not vary significantly. Closed systems differ

because SO_4^{2-} consumption exceeds supply (Gomes & Hurtgen, 2013; 2015). In these

systems, H_2S is the dominant sulfur species and SO_4^{2-} concentrations can be very low

(Anderson et al., 1988). As sulfate concentrations decrease the $\delta^{34}S$ of the sulfide

produced from BSR approaches that of the initial SO_4^{2-} input into the lake (+20 to 30‰)

(Rees, 1972; Sælen et al., 1993; Gomes & Hurtgen, 2013; 2015) (Figure 10).

Replenishment is the difference between open and closed systems is SO_4^{2-}. In

open systems, sulfur isotope fractionation follows a linear pattern and the $\delta^{34}S$ of SO_4^{2-}

changes at the same rate as does S^{2-} (Figure 10b). In closed systems, sulfur isotope

fractionation between the sulfate and sulfide generally follows a non-linear pattern, which

is dependent on the extent of re-oxidation; SO_4^{2-} becomes more and more enriched in S^{34}

as the SO_4^{2-} concentration approaches zero. $\delta^{34}S$ values of SO_4^{2-} and S^{2-} in the water

column reach their highest values in the super-anoxic zone due to low SO_4^{2-}

concentrations (Figure 10a). The trends observed in $\delta^{34}S$ values of sulfides in closed

basins occur because of the "reservoir effect" in a closed system (Anderson et al., 1988;

Sælen et al., 1993; Gomes & Hurtgen, 2013; 2015). Figure 10 shows instantaneous $\delta^{34}S$

values of sulfide. In this study, time averaged $\delta^{34}S$ values are being examined.

Therefore, it is possible for sulfide formed later on and preserved in the pyrite to have

and even higher $\delta^{34}S$ value than the input sulfate, as it is depleted in order to compensate

for the low $\delta^{34}S$ values of sulfide formed under higher sulfate concentrations.

Reservoir effects affect both high-SO_4^{2-} (Sælen et al., 1993; Zerkle et al., 2010)

and low-SO_4^{2-} systems (Gomes & Hurtgen, 2013; 2015); however they are likely to have

a greater impact on low-SO_4^{2-} systems. In low-SO_4^{2-} systems like Lake McCarrons, the

relatively large fractions imparted during sulfur cycling cause sulfate at depth to

have relatively high δ^{34}S values compared to those for sulfate closer to the surface (Sælen et al., 1993; Gomes & Hurtgen, 2013). As the SO_4^{2-} becomes more enriched in ^{34}S with depth, the associated S^{2-} produced is relatively enriched in ^{34}S as well. Total SO_4^{2-} consumption will produce a pool of pyrite having δ^{34}S values similar to the input SO_4^{2-} value.

Lakes have shorter residence times than the ocean, therefore SO_4^{2-} concentrations in the Newark Basin Triassic lake were likely much lower than marine concentrations (~28mM) perhaps even as low as that of present day Lake McCarrons (~200 μM) (Gomes & Hurtgen, 2013). If the Triassic lake was similar to present-day Lake McCarrons, which had an oxic-euxinic boundary at ~12 m depth and a total depth of ~17 m, euxinic conditions were present in relatively shallow lakes (Gomes & Hurtgen, 2013). In a relatively deep lake with euxinic conditions, pyrite formation occurs in the water column or very close to the sediment-water interface where sulfate concentrations are low, and as a result the pyrite has a relatively high δ^{34}S because sulfate concentrations dampen BSR associated fractionation effects (Figure 11) (Gomes & Hurtgen, 2013; 2015, Sælen et al., 1993). When the water column is oxic, pyrite forms deeper in the sediments because of more bottom water circulation and rapid reaction of H_2S with iron oxides as observed in Framvaren Fjord (Sælen et al., 1993). High concentrations of sulfate in bottom and sediment pore waters of shallow water bodies result in the larger fractionations associated with BSR cause the preserved pyrite to have a low δ^{34}S (Figure 11). Additionally, the lake depth influences pyrite grain size which could affect the δ^{34}S value of the grain. Zhu (2010) showed that pyrite concentrations were highest in the deepest lake environments in the Newark Basin, leading to a conclusion that the pyrite grains are much smaller or

inconsistently deposited in the deep lake environments. Smaller grains are formed over a

shorter period of time and would therefore represent an average $\delta^{34}S$ for a shorter amount

of time than a large grain. While this is important to note, there was no grain size

discrimination in this study, therefore, any bias was negated by random grain size

sampling.

The results indicate that pyrite formed in a deep lake environment (depth rank >1)

have relatively high $\delta^{34}S$ values (Table 2). An interesting exception is found in one deep

lake sample (NB31), which had an anomalously low $\delta^{34}S$ value of -11.22‰. This sample

corresponds to the early stages of a shallow to deep lake transition and may indicate that

the sulfur cycle did not respond to changes at the same rate that lake changed. Most

pyrite formed in a shallow lake (depth rank $\leq$ 1) (Figure 9) have $\delta^{34}S$ values that fall in

the range of -5 to +1‰. While most of the samples are negative, some samples

(CC25PYR2, NB7, NB46, NB47) had positive $\delta^{34}S$ values (greater than +3‰). The

variations in $\delta^{34}S$ in shallow lake could be caused by annual to decadal variations in the

redox conditions or sulfate concentration of the Newark Basin Triassic lake that were

superimposed on the longer-term patterns driven by precession.

Sample NB7 at 908.86 m (2981.85 ft.) is another outlier, recording a large

positive isotope excursion of ~19‰ between 909.25 and 908.86 m (NB12 and NB7).

The depth ranking for NB7 is 0.75 indicating that the lake was a frequently a playa lake

which at some points may have dried out completely. One possible explanation for the

anomalous value of NB7 (+19.4‰) is an ephemeral period of low SO_4^{2-} concentration

during the time of deposition. As a result of the reservoir effect, a low SO_4^{2-}

concentration in the playa would lower the magnitude of fractionation associated with BSR if nearly all of the sulfate entering the lake was reduced (Kemp & Thode, 1986).

Pyrite formed in a lake with a certain depth at a certain time may not consistently have the same isotope value as a grain deposited in a lake with a similar depth at a different time. Sample CC22PYR1, with a depth ranking of 3.5, recorded a $\delta^{34}S$ of +7.5‰. Sample NB44, also deposited in a lake with a depth ranking of 3.5 had a $\delta^{34}S$ of +0.42‰. This difference may be caused by a change in either the SO_4^{2-} flux or the amount or type of organic matter in the sediments. Nonetheless, a consistent pattern is still seen, as these grains were both deposited in relatively deep lakes with ^{34}S rich, euxinic, bottom waters and have relatively high $\delta^{34}S$ values.

7. Conclusion

The depth of a lake controls its sulfur geochemistry through its influence on the development of the euxinic zone, and the location of where pyrite forms: in the water column or sediment water interface (deep lake) or in the sediments (shallow lake). The lake level also determines the concentration of SO_4^{2-} in the environment where pyrite forms. Holding other factors such as iron and organic matter availability constant, changes in the sulfur isotope values of lacustrine pyrite should change systematically as the lake level rises and falls and the relative values should indicate the dominant mechanism of pyrite formation in the system.

The Triassic Lake in the Newark Basin provides a robust record of climatic forcing of lake level fluctuation and its effect on lacustrine geochemistry. The results of this study are in accordance with sulfur isotope studies of modern day high- and low-

sulfate systems. This study has shown how a closed geochemical system can evolve over time due to physical processes. In this case, movement of the chemocline affected the location and speed of microbial sulfur metabolism, which can be observed in the sulfur isotope values of the pyrite in the sediments.

As supported by previous studies, pyrite formation in deep lakes with euxinic zones occurs in the water column or at the sediment-water interface. Pyrite formed in these settings have a unique isotope signature because of the reservoir effect and low SO_4^{2-} concentrations, which influence BSR and furthermore the isotopic signature imparted by the process. In shallow lakes, pyrite forms in the sediment which is overlain by oxic water with a relatively high concentration of SO_4^{2-} because of it is less diluted than a deeper lake.

Using $\delta^{34}S$ values of pyrite and depth rankings of sedimentary rock core sections, this study shows how lake level may have affected the sulfur isotope systematics of the Newark Basin Triassic lake. Further work is needed to fully understand the sulfur isotope systematics of this system with a particular focus on the deepest lakes where pyrite was difficult to find in the sections studied here. Analyzing pyrite across several Van Houten cycles from a different range of depths in the core would reveal how the sulfur cycle in the lake changed over a longer period of time and would also shed light on the variability of $\delta^{34}S$ values for pyrite formed in similar environments with the same depth rank.

8. References

Anderson L.G., Dyrssen D., & Hall P.O.J. (1988) On the Sulphur chemistry of a super anoxic fjord, Framvaren, south Norway. *Marine Chemistry*, **23**, 283-293.

Appold M., Kesler S.E., Alt J.C. (1995) Sulfur isotope and fluid inclusion constraints on the genesis of Mississippi Valley-type mineralization in the central Appalachians. *Economic Geology*, **90**, 902-919.

Ault W.U. & Kulp J.L. (1960) Sulphur isotopes and ore deposits. *Economic Geology*, **55**, 73-100.

Bak F. & Cypionka H. (1987) A novel type of energy metabolism involving fermentation of inorganic Sulphur compounds. *Nature*, **326**, 891-892.

Bak F. & Pfenning N. (1991) Microbial sulfate reduction in littoral sediment of Lake Constance. *FEMS Microbiology Ecology*, **85**, 31-42.

Benson L.V. (1981) Paleoclimatic significance of lake-level fluctuations in the Lahontan Basin. *Quaternary Research*, **16**, 3, 390-403.

Canfield D.E. (2000) Isotope fractionation by natural populations of sulfate-reducing bacteria. *Geochimica et Cosmochimica Acta,* **65**, 7, 1117-1124.

Chambers L.A., Trudinger P. A., Smith J. W., & Burns M. S. (1975) Fractionation of sulfur isotopes by continuous cultures of *Desulfovibro desulfuricans*. *Canadian Journal of Microbiology*, **21**, 1602-1607.

Canfield D.E. & Des Marais D.J. (1991) Aerobic sulfate reduction in microbial mats. *Science Reprint Series*, **251**, 1471-1473

Crawford M.J. & Beales F.W. (1983) The Shawanagunk mine: A possible sandstone-hosted Mississippi Valley type deposit in New York. In: International conference on Mississippi Valley type lead-zinc deposits (Eds. Kisvara, G., Grant, S.K., Pratt, W.P. & Koenig, J.W.) Proceedings volume: Rolla, University of Missouri-Rolla Press, 436-446.

Devereaux R., Delaney M., Widdel F., & Stahl D. A. (1989) Natural relationships among sulfate-reducing eubacteria. *Journal of Bacteriology*, **171**, 6689-6695.

Dilling W. & Cypionka A. (1990) Aerobic respiration in sulfate-reducing bacteria. *FEMS Microbiology Letters*, **71**, 123-128

El-Tabakh M. (1994) Early Rift-basin Deposition: Triassic-Jurassic Sedimentation and Subsequent Diagenesis in the Newark Basin, New Jersey. PhD. Dissertation, City University of New York.

Eschmann A., Kühl M., & Cypionka H. (1999) Aerotaxis in *Desulfovibro. Environmental Microbiology*, **1**, 489-494.

Fry B., Cox J., Gest H. and Hayes J.M. (1986) Discrimination between $\delta^{34}S$ and ^{32}S during bacterial metabolism of inorganic sulfur compounds. *Journal of Bacteriology*, **165**, 328-330.

Fry B. Gest H. & Hayes J.M. (1984) Isotope effects associated with the anaerobic oxidation of sulfide by the purple photosynthetic bacterium, *Chromatium vinosum. FEMS Microbiology Letters*, **22**, 283-287.

Fry B., Gest H., & Hayes J.M. (1985) Isotope effects associated with the anaerobic oxidation of sulfite and thiosulfate by the photosynthetic bacterium, *Chromatium vinosum. FEMS Microbiology Letters*, **27**, 227-232.

Gomes M.L. & Hurtgen M.T. (2013) Sulfur isotope systematics of a euxinic, low-sulfate lake: Evaluating the importance of the reservoir effect in modern and ancient oceans. *Geology*, **41**, 6, 663-666.

Gomes M. L. & Hurtgen M.T. (2015) Sulfur isotope fractionation in modern euxinic systems: Implications for paleoenvironmental reconstructions of paired sulfate–sulfide isotope records. *Geochimica et Cosmochimica Acta* **157**, 39-55.

Harrison A.G. & Thode H.G. (1958) Mechanism of the bacterial reduction of sulphate from isotope fractionation studies. *Transactions of the Faraday Society*, **54**, 84-92.

Habicht K.S., Canfield D.E., Rethmeier J. (1998) Isotope fractionation during bacterial reduction and disproportionation of thiosulfate and sulfite. *Geochimica et Cosmochimica Acta*, **62**, 15, 2585-2595.

Holmer M. & Storkholm P. (2001) Sulphate reduction and Sulphur cycling in lake sediments: a review. *Freshwater Biology*, **46**, 431-451.

Holser W.T., Schidlowski M., Mackenzie, F.T., & Maynard, J.B. (1988) Geochemical cycles of carbon and sulfur. In Chemical Cycles in the Evolution of the Earth (Eds. Gregor C.B., Garrels R.M., Mackenzie F.T., Maynard J.B.) Wiley, New York, 105-173.

Howe S.S. (1981) Mineralogy, fluid inclusions, and stable isotopes of lead-zinc occurrences in central Pennsylvania. Master's Thesis, The Pennsylvania State University, 155 p.

Ivanov M.V., Gogotova G.I., Matrosov A.G., & Zyakun A.M. (1976) Fractionation of sulfur isotopes by phototrophic sulfur bacteria. *Microbiology*, **45**, 655-659.

Janssen P.H., Schuhmann A., Bak F., & Liesack W. (1996) Disproportionation of inorganic sulfur compounds by the sulfate-reducing bacterium *Desulfocapsa thiozymogenes* gen. nov., sp. Nov. *Archives für Microbiologie*, **66**, 184-192.

Jones G.E. & Starkey R.L., (1957) Fractionation of stable isotopes of sulfur by micro-organisms and their role in deposition of native sulfur. *Applied Microbiology*, **5**, 111.

Jørgensen B.B. (1988) Ecology of the sulphur cycle: oxidative pathways in the sediment. In: *The Nitrogen and Sulphur Cycles* (Eds J.A. Cole & S.J. Ferguson), Cambridge University Press, Cambridge, 31-63

Jørgensen B.B. (1990) The sulfur cycle of freshwater sediments: Role of thiosulfate. *Limnology and Oceanography,* **35**, 1329-1342.

Jørgensen B.B. & Bak F. (1991) Pathways and microbiology of thiosulfate transformations and sulfate reducing in a marine sediment (Kattegat, Denmark). *Applied Environmental Microbiology*, **57**, 847-856.

Kaplan I.R. & Rittenberg S.C. (1964) Microbiological fractionation of Sulphur isotopes. *Journal of General Microbiology,* **34**, 195-212

Kemp A.L.W. & Thode H.G. (1968) The mechanism of the bacterial reduction of sulphate and of suphite from isotope fractionation studies. *Geochimica et Cosmochimica Acta*, **32**, 71-91.

King G.M. & Klug M.J. (1982a) Comparative aspects of sulfur mineralization in sediments of a eutrophic lake basin. *Applied Environmental Microbiology*, **43**, 14036-1412.

LeHuray A.P. (1984) Lead- and sulfur-isotope systematics in some sulfide deposits of the Piedmont and Blue Ridge provinces of the southern Appalachians, U.S.A. *U.S. Geological Survey Open-File Report*, **84-112**, 429.

Manspeizer W. (1982) Triassic-Liassic basins and climate of the Atlantic passive margins. *Geologische Rundschau*, **71,** 3, 895-917.

Marschall C., Frenzel P., and Cypionka H. (1993) Influence of oxygen on sulfate reduction and growth of sulfate-reducing bacteria. *Archives of Microbiology*, **159**, 168-173.

McLaughlin D.B. (1933) A note on the stratigraphy of the Brunswick Formation (Newark) in Pennsylvania. Michigan Academy of Science, Arts, and Letters, **18**, 59-74.

McLaughlin D.B. (1946b) Continuity of strata in the Newark Series. Michigan Academy of Science, Arts, and Letters, **32**, 295-303.

Newton R. & Bottrell S. (2007) Stable isotopes of carbon and sulphur as indicators of environmental change: past and present. *Journal of the Geological Society, London*, **164**, 691-708.

Nriagu J.O. & Soon Y.K. (1985) Distribution and isotopic composition of sulfur in lake sediments of northern Ontario. *Geochimica et Cosmochimica Acta*, **49**, 823-834.

Olsen P.E. (1978) On the use of the term Newark for Triassic and Early Jurassic rocks in eastern North America. *Newsletters on Stratigraphy*, **7**, 2, 90-95.

Olsen P.E. (1984b) Periodicity of lake-level cycles in the Late Triassic Lockatong Formation of the Newark basin. In: Milaknovitch and climate, Part1 (Eds Berger, A. et al.). Boston, Massachusettes, D. Reidel Publishing Company, 129-146.

Olsen P.E. (1986) A 40-million year lake record of early Mesozoic orbital climatic forcing. Science, **234**, 4778, 842-848.

Olsen P.E. & Kent D. V. (1995) Milankovitch climate forcing in the tropics of Pangaea during the Late Triassic. *Palaeogeography, Palaeoclimatology, Palaeoecology*, **122**, 1-26.

Olsen P.E. & Kent D. V., Cornet, B., Witte, W. K., Schlishce, R. W. (1996) High-resolution stratigraphy of the Newark rift basin (early Mesozoic, eastern North America). *GSA Bulletin*, **108**, 1, 40-77.

Pazzaglia F.J. & Brandon M.T. (1996) Macrogeomorphic evolution of the post-Triassic Appalachian mountains determined by deconvolution of the offshore basin sedimentary record. *Basin Research*, **8**, 255-278.

Rees C.E. (1973) A steady-state model for Sulphur isotope fractionation in bacterial reduction processes. *Geochimica et Cosmochimica Acta*, **37**, 1141-1162.

Rickard D.T. (1969) The chemistry of iron sulfide formation at low temperatures. Stockholm Contributions in Geology, **20**, 67-95.

Rudd J.W.M. & Kelly C.A., Furutani A. (1986) The rold of sulfate reduction in long term accumulation of organic and inorganic sulfur lake sediments. *Limnology and Oceanography*, **31**, 6, 1281-1291.

Sass H., Cypionka H., & Babenzien H. D. (1997) Vertical distribution of sulfate-reducing bacteria at the oxic-anoxic interface in sediments of the oligotrophic Lake Stechlin. *FEMS Microbiology Ecology*, **22**, 245-255.

Sælen, G. Raiswell R., Talbot M.R., Skei J.M., & Bottrell S.H. (1993) Heavy sedimentary sulfur isotopes as indicators of super-anoxic bottom-water conditions. *Geology*, **21**, 1091-1094.

Schlische R.W. (1992) Structural and stratigraphic development of the Newark extensional basin, eastern North America: Evidence for the growth of the basin and its bounding structures. *Geological Society of America Bulletin*, **104**, 1246-1263.

Van Houten F.B. (1964). Cyclic lacustrine sedimentation, Upper Triassic Lockatong Formation, central New Jersey and adjacent Pennsylvania. In: Symposium on Cyclic Sedimentation (O.F. Mermaid Ed). Kansas Geological Survey Bulletin, **169**, 497-531.

Witte W.K. & Kent D.V. (1990) The palegomagnetism of redbeds and basalts of the Hettagian extrusive zone, Newark basin. *Journal of Geophysical Research*, **95**, 17533-17546

Wilbur J.S., Mutschler F.E., Friedman J.D., & Zartman R.E. (1990) New chemical, isotopic, and fluid inclusion data from zinc-lead-copper veins, Shawanagunk Mountains, New York. *Economic Geology*, **85**, 182-196.

Yatsu, E. (1988). The nature of weathering: an introduction. Sozosha, Tokyo, Japan.

Zerkle A.L., Kamyshnh A., Jr., Kump L.R., Farquhar J., Oduro H. & Arthur M.A. (2010) Sulfur cycling in a stratified euxinic lake with moderately high sulfate: Constraints from quadruple S isotopes. *Geochimica et Cosmochimia Acta*, **74**, 4953-4970.

Zhu, W. (2010) Chemical and microbial control of pyrite weathering and its implications to arsenic mobility and sulfur and iron geochemistry. Master's Thesis, Rutgers University, New Brunswick.

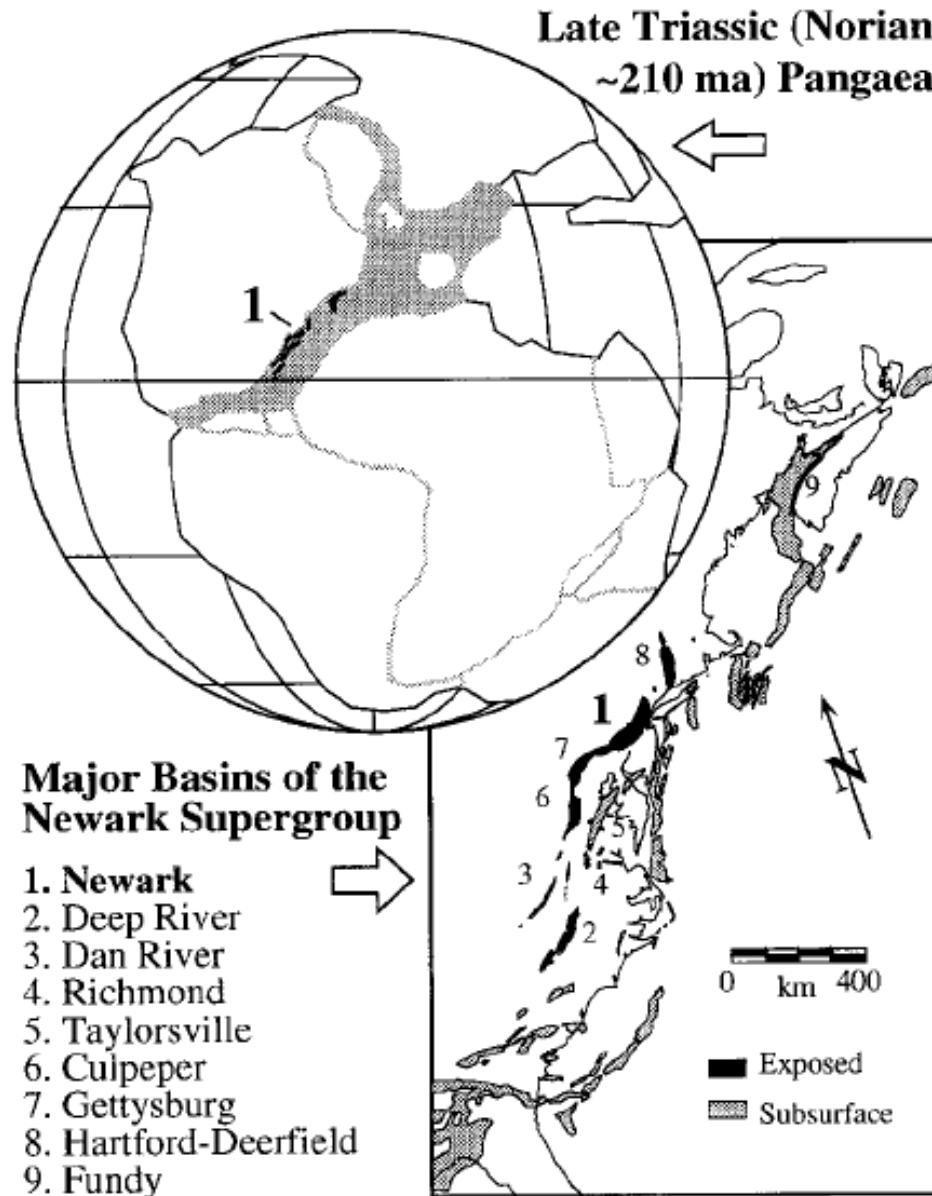| Depth Rank	Sedimentary Fabric	Description	Environment of deposition
0	Intense breccia fabric	Massive mudstones with densely superimposed, jagged cracks often with small cement-filled vugs in the cracks with little original bedding visible. Often appears as nearly featureless	Mostly dry playa mudflats and aggrading playa mudflats
1	Breccia fabric	Massive mudstones with superimposed, jagged cracks with distinct clumps of matrix with original bedding preserved.	Very frequently dry playas
2	Mudcracked mudstone	Thin-bedded mudstone with jagged or more frequently sinuous cracks. Pinch and swell lamination frequently present in matrix between cracks	Lakes with rapid depth fluctuations, sometimes saline, commonly drying out. Can be margin of relatively deep lake.
3	Thin-bedded non-mudcracked mudstone	Thin bedded to massive mudstone, often with >1% total organic carbon. Pinch and swell lamination and small burrows locally abundant. Cracks absent. Fish fragments sometimes present.	Relatively shallow perennial lakes or the margins of relatively deep lakes.
4	Finely laminated mudstone	Mudstone with usually discontinuous laminae (<1 mm thick). Pinch and swell lamination and burrows rare. Fragmentary to complete fossil fish can be present and total organic carbon content often >2%.	Relatively deep perennial lake.
5	Micro-laminated Mudstone	Mudstone with continuous micro laminae (<1 mm thick). No burrows. Complete fossil fish often abundant. Total organic content often >3%.	Deep lake.

Table 1. Depth ranking criteria

A table listing the depth rankings, the criteria for assigning depth ranking to a core depth, and the interpreted environment of deposition; modified from Olsen & Kent, 1996.

| Sample Name	Core Depth (m)	Core Depth (ft.)	Depth Rank	Color	Lithology	δ^{34}S (‰)
NB3	908.24	2979.79	0.75	Purple	Fine sandstone	-1.35±0.36
NB7	908.87	2981.85	0.75	Purple	Fine sandstone	19.37±0.31
NB12	909.25	2983.10	0.75	Purple	Fine sandstone	0.82±0.28
NB16	910.60	2987.54	0.25	Red	Siltstone	-4.75±0.57
NB19	911.52	2990.55	0.25	Red	Siltstone	-4.46±0.84
CC25PYR2	912.64	2994.21	0.25	Red	Siltstone	3.05±4.30
NB25	913.74	2997.85	1	Gray	Siltstone	3.29±1.27
CC22PYR1	914.97	3001.87	3.5	Dark Gray	Siltstone	7.49±0.15
NB30	915.42	3003.74	2.5	Dark Gray	Siltstone	10.79±0.03
NB31	915.63	3004.02	2.5	Dark Gray	Siltstone	-11.22±1.88
NB33	916.18	3005.83	0	Gray	Mudstone	-4.00±0.39
NB34	916.89	3008.16	0	Purple	Mudstone	-5.05±0.15
NB35	917.21	3009.22	0	Purple	Siltstone	0.17±0.18
NB36	917.98	3011.75	0	Purple	Siltstone	-0.67±0.17
NB37	918.26	3012.67	0	Gray	Fine sandstone	-2.73±0.46
NB38	919.00	3015.08	0.5	Gray	Fine sandstone	2.22±1.63
NB39	920.33	3019.44	0.5	Gray	Fine sandstone	-3.82±0.23
NB40	921.37	3022.87	0	Purple	Mudstone	-0.58±2.91
NB41	922.42	3026.31	0.5	Red	Mudstone	0.99±0.33
NB42	923.58	3030.11	0.5	Gray	Fine sandstone	3.16±0.17
NB43	925.61	3036.79	2.5	Grey	Mudstone	-1.02±0.26
NB44	925.84	3037.53	3.5	Dark Gray	Siltstone	0.42±0.23
NB46	928.50	3046.25	0	Gray	Mudstone	6.23±0.97
NB47	928.99	3047.9	0	Gray	Mudstone	3.76±0.45

Table 2. Pyrite Samples

Names, core depths, depth ranking, color, lithology, and δ^{34}S values of pyrite samples from the Nursery #1 core. δ^{34}S values are means ± 1 standard deviation for duplicate samples. Depth rank, color, and lithology obtained from the NBCP database http://www.ldeo.columbia.edu/~polsen/nbcp/nbcp.html.

Late Triassic (Norian ~210 ma) Pangaea

Major Basins of the Newark Supergroup

1. Newark
2. Deep River
3. Dan River
4. Richmond
5. Taylorsville
6. Culpeper
7. Gettysburg
8. Hartford-Deerfield
9. Fundy

0   km   400

■ Exposed
▨ Subsurface

Figure 1. Late Triassic paleogeography of the Newark Basin

Figure 1. A reconstruction of Pangea during the late Triassic showing the zone of early Mesozoic rifting (shaded) and the basins of the Newark Supergroup (black) and the early Mesozoic rift basins of eastern North America (inset) today. From Olsen et al., 1996.
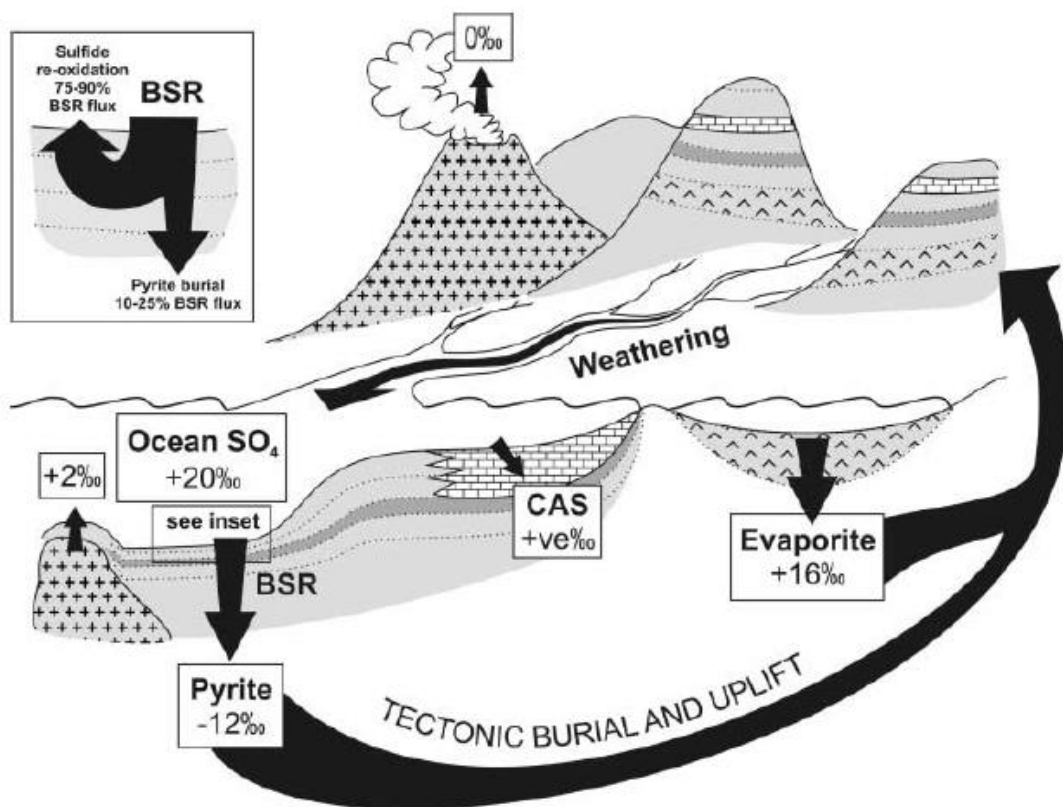
Figure 2. Global sulfur cycle

A schematic diagram of the global sulfur cycle and the isotopic compositions of each reservoir (CAS = Carbonate Associated Sulfate) from Newton and Bottrell, 2006.
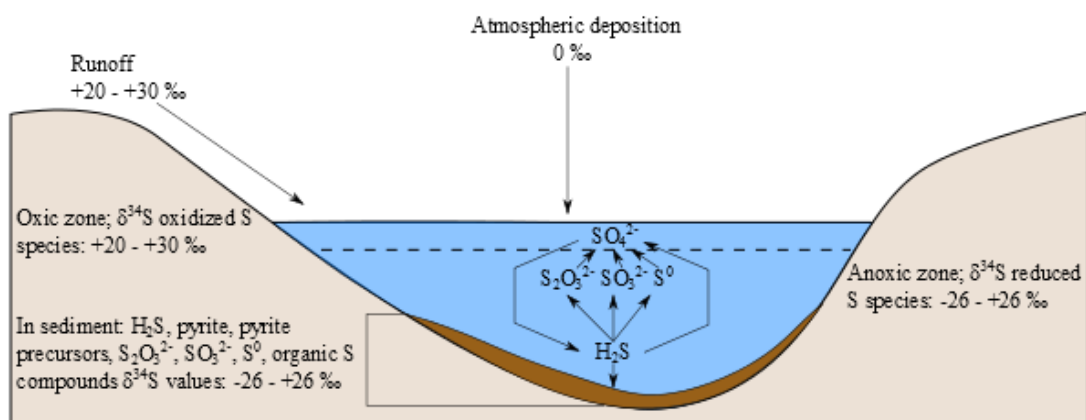
Figure 3. Newark Basin Triassic Lake sulfur cycle

A schematic diagram of the sulfur cycle in the Newark Basin Triassic lake and the sulfur isotope value associated with each reservoir. Arrows indicate fluxes and redox reactions.
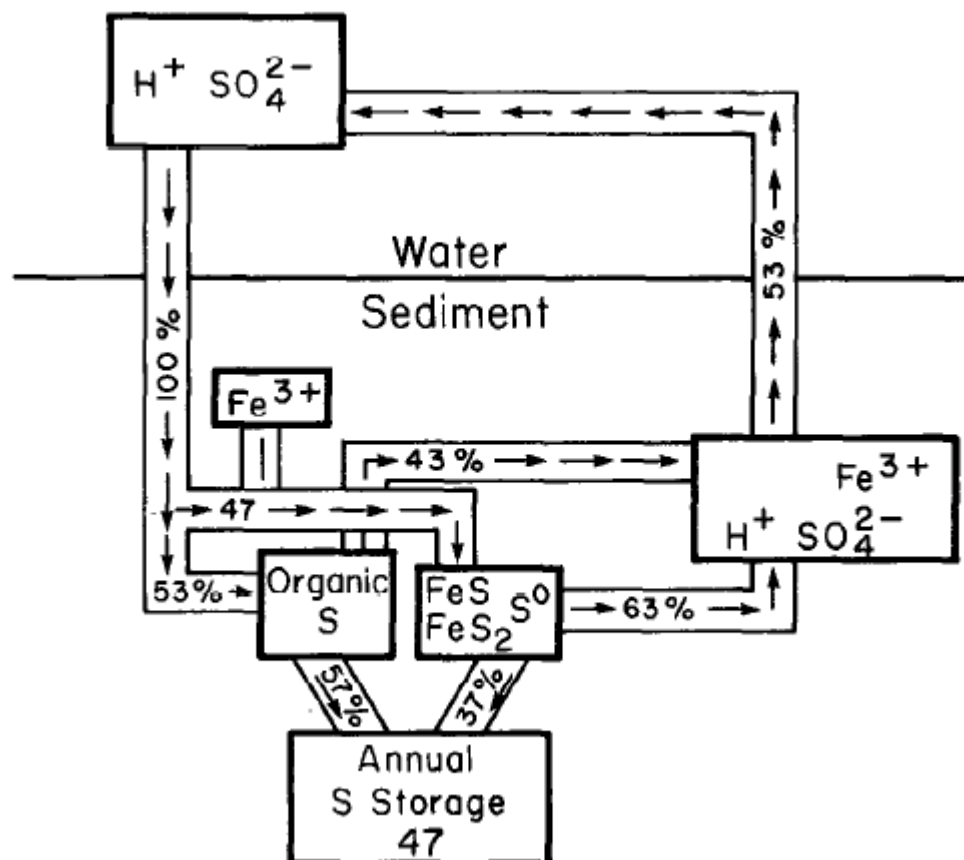
Figure 4. Sedimentary sulfur reservoirs and fluxes

The reservoirs of sulfur at the sediment water interface in a lacustrine setting. Numbers represent the percent of the original sulfate that goes to each reservoir. From Rudd et al., 1986.
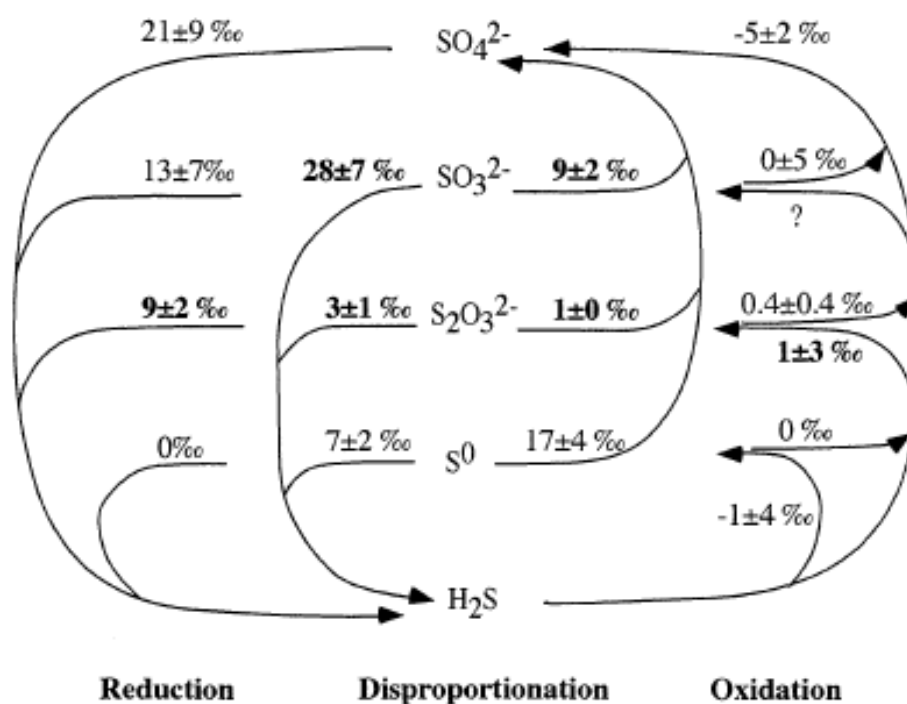
Figure 5. Isotope effects on sulfur of microbial processes

The isotope effects associated with the microbial reduction (left column), disproportionation (middle column), and oxidation (right column) of various sulfur species present in the environment. From Habicht et al. 1998.
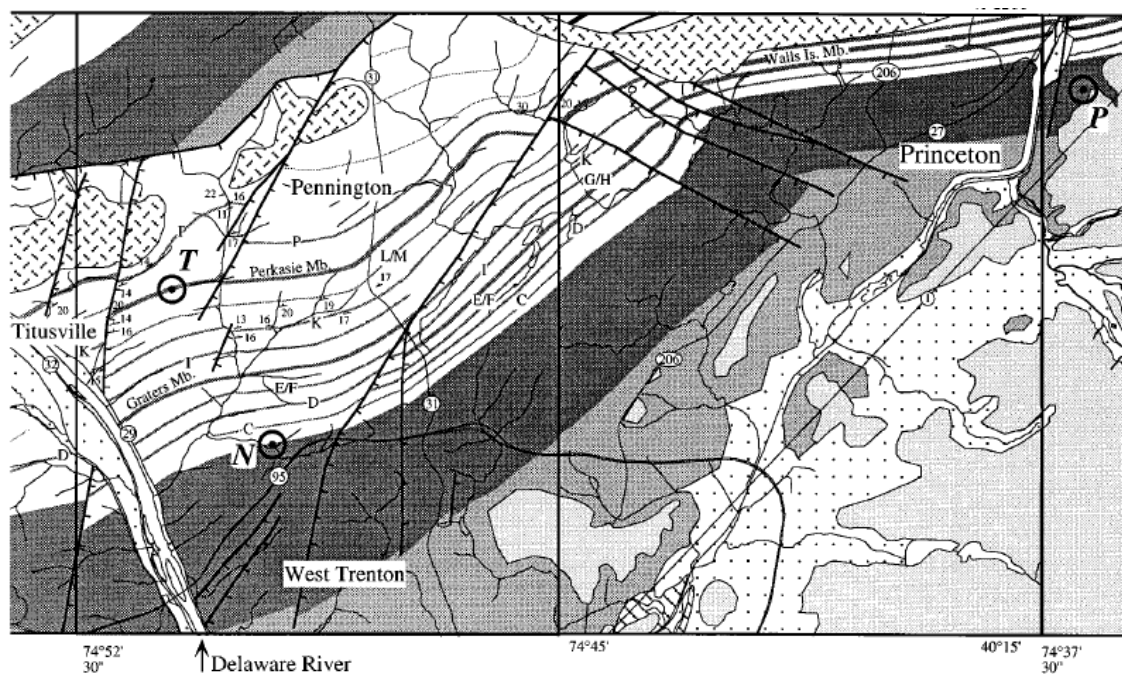
Figure 6b.
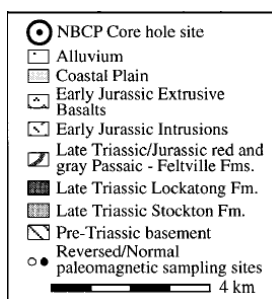
Figure 6. Location of the Nursery #1 core

Figure 6. (a) Map of the Titusville, NJ to the Princeton, NJ area (b) key to units and scale. Nursery core taken from core site "N." From Olsen et al. 1996.
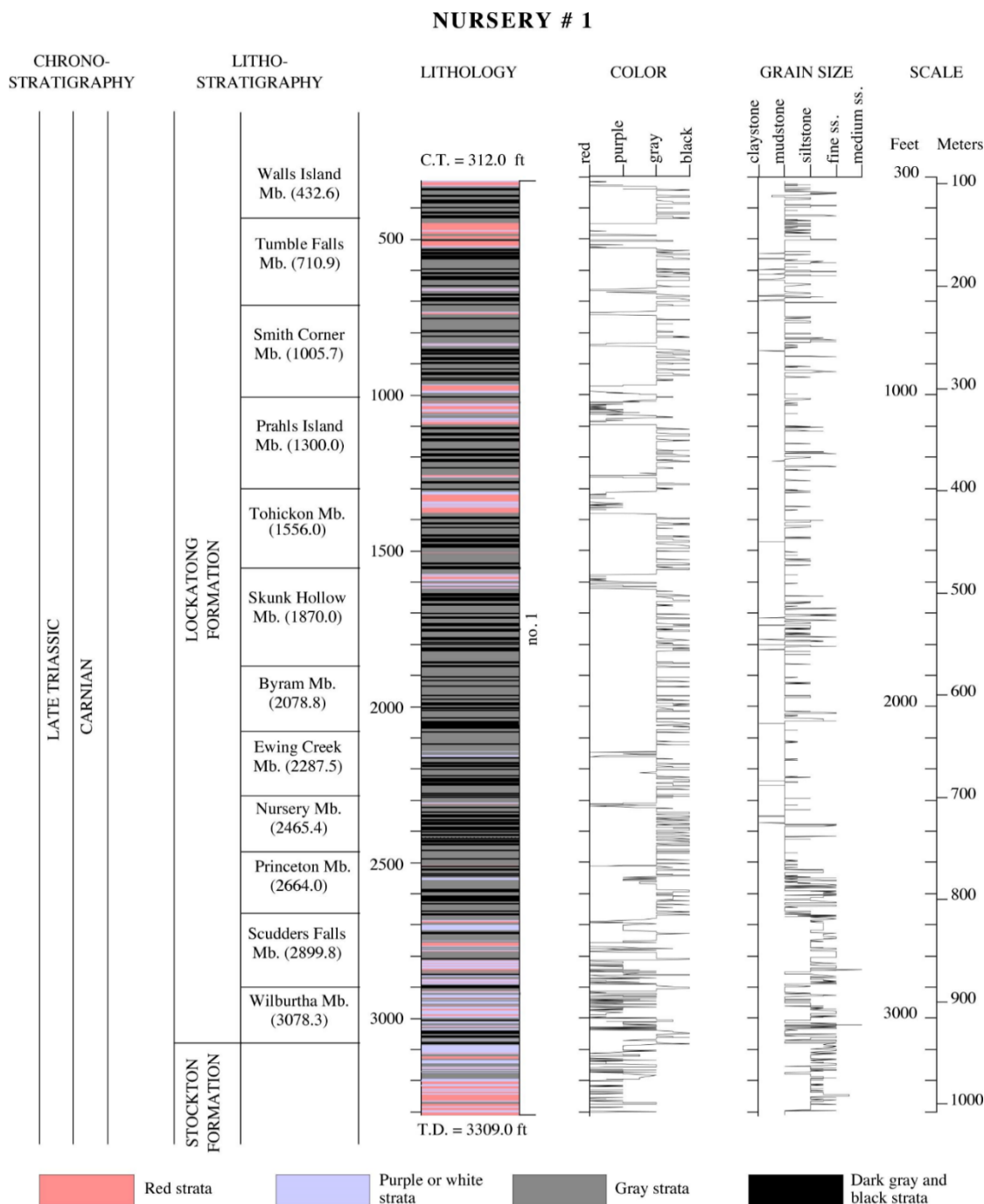
Figure 7. Stratigraphy of the Nursery #1 Core (a) and pyrite sample depths (b)

Figure 7a. (above) Stratigraphic log of the Nursery #1 core showing age, stratigraphy, color, grain size, and core depth in feet, (from Olsen et al. 1996)
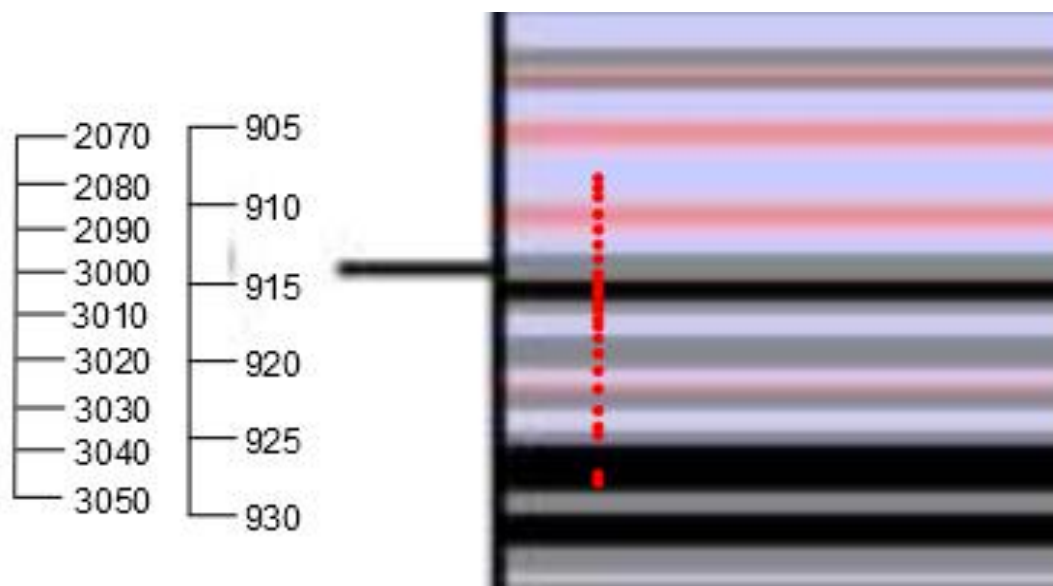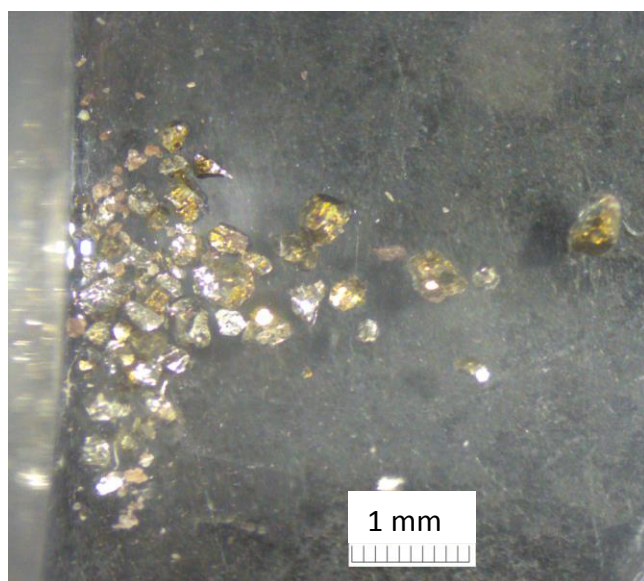
Figure 7b. Close up of ~900 m (3000 ft.) core depth in the Nursery #1 core; locations of pyrite samples used in this study indicated by red dots; left scale in feet, right in meters; modified from Olsen et al, 1996.
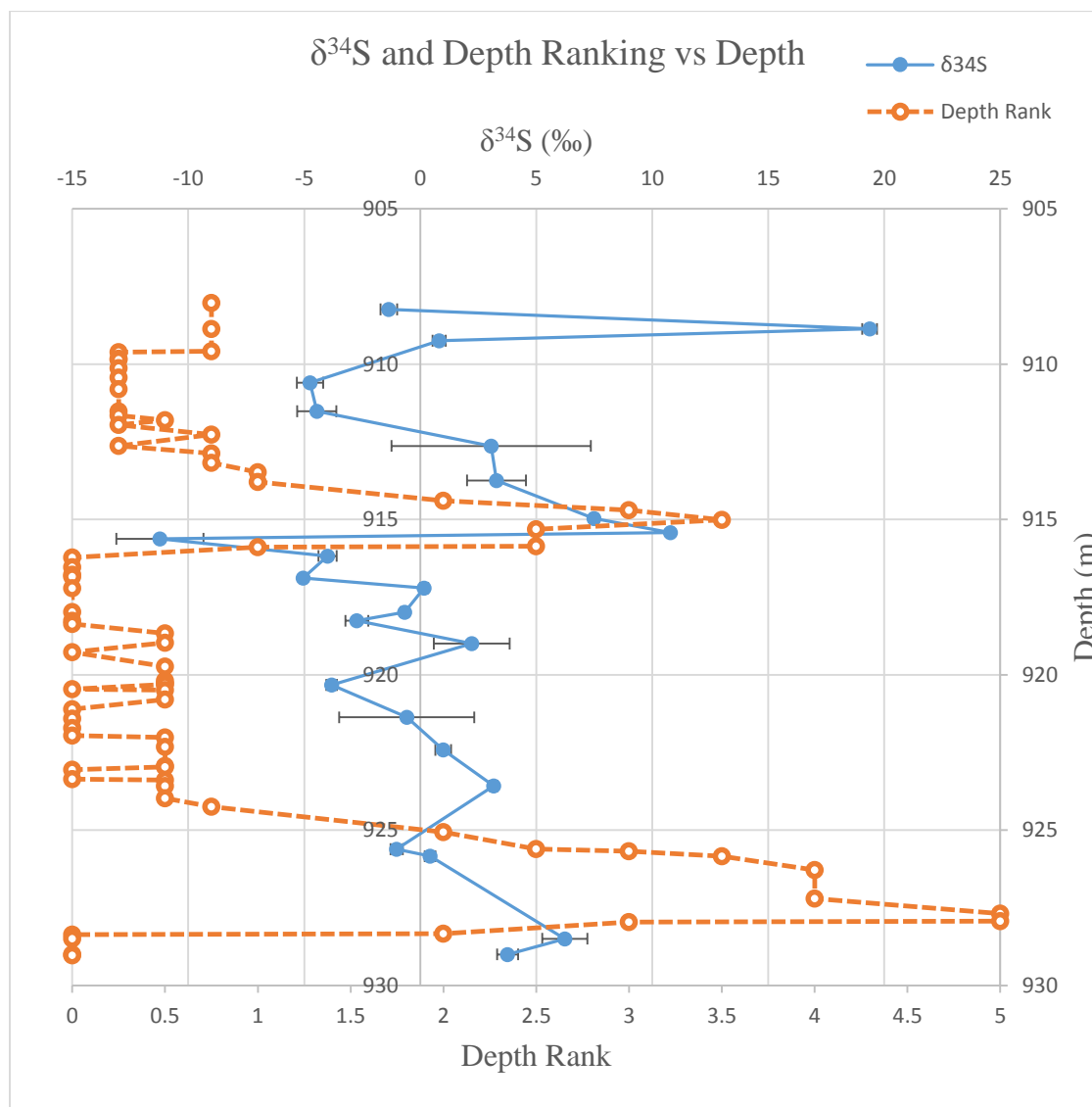
a)
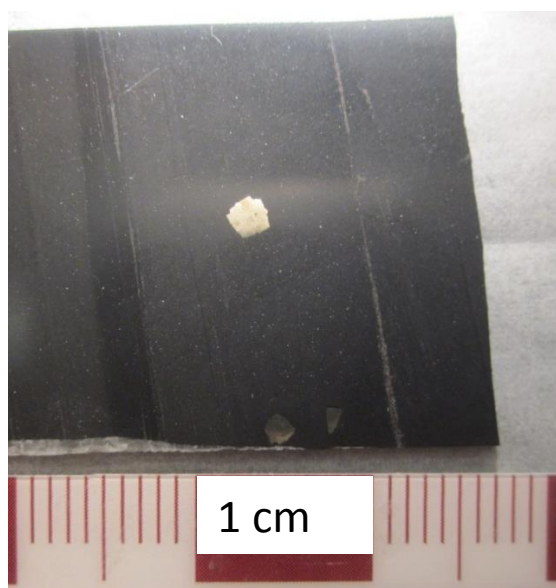
b)

Figure 8. Pyrite samples

Pyrite samples from the Nursery #1 core. Scale in 8a is 1 centimeter, scale in 8b is 1 millimeter.

Figure 9. δ³⁴S values of pyrite and depth rank versus depth in the Nursery #1 core section

A plot of δ³⁴S values of pyrite ($\delta^{34}S_{pyr}$) from Newark Basin Triassic mudstones and paleolake depth rank vs. depth in the Nursery #1 core section. Error bars for each sample reflect the range of δ³⁴S values in multiple grains from the same sample.
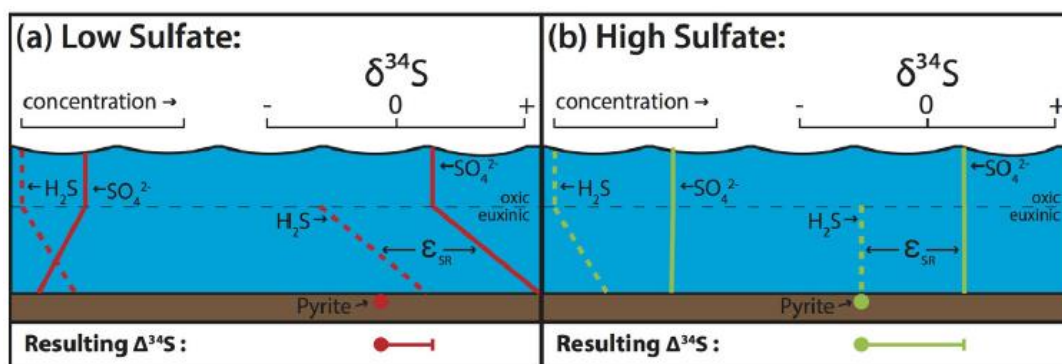
Figure 10. The reservoir effect in low and high sulfate systems

A diagram illustrating the reservoir effect and its effect on $\delta^{34}S$ values of sulfate and sulfide in (a) a low sulfate and (b) high sulfate system. In each panel the concentration (left) and $\delta^{34}S$ value of sulfide (H_2S, dashed line) and sulfate (SO_4^{2-}, solid line) are plotted with depth in the water. The $\delta^{34}S$ value of pyrite (filled circle) is approximated as the average water column $\delta^{34}S$ of sulfide. The difference between $\delta^{34}S$ values for sulfate and preserved sulfide are projected down into the lower box as the line between the $\delta^{34}S$ of pyrite and $\delta^{34}S$ of sulfate at the top of the water column. From Gomes and Hurtgen, 2015.

[Species] δ^{34}S   [Species] δ^{34}S [Species] δ^{34}S [Species] δ^{34}S
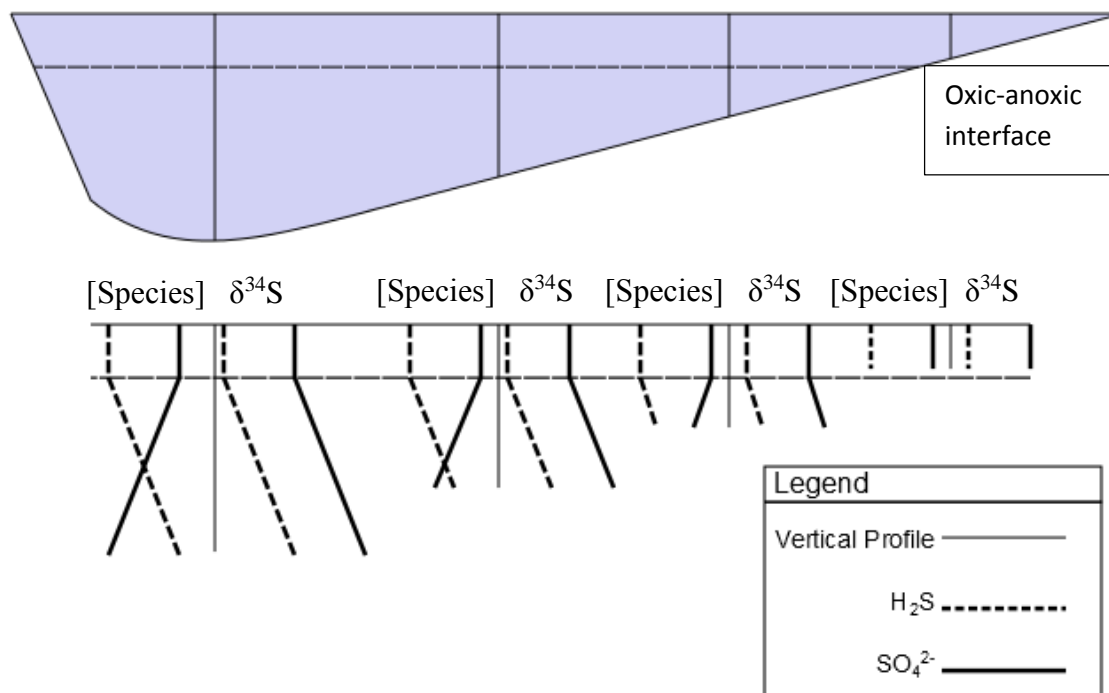
Figure 11. Model of lake environments, sulfur species, and isotope systematics in the Triassic Lake

A diagram showing vertical profiles of the Triassic Newark Basin lake in deep (left) to progressively more shallow (right) environments. Water column is oxic above oxic-anoxic interface and anoxic below. Graphs below the lake diagram show vertical profiles of relative sulfate (solid line) and sulfide (dashed line) concentrations (left sides of the graphs) and relative δ^{34}S values of the species (right sides of the graphs) at each of the locations.